An intercomparison between low-frequency variability indices

P. Bongioannini Cerlini, S. Corti & S. Tibaldi

Published online: 27 Jan 2017.

Submit your article to this journal ↗

Article views: 13

Citing articles: 6 View citing articles ↗

An intercomparison between low-frequency variability indices

By P. BONGIOANNINI CERLINI[1]*, S. CORTI[2] and S. TIBALDI[3], [1]*Department of Earth and Geo-Environmental Sciences, Via Zamboni 67, University of Bologna, Bologna, Italy;* [2]*CINECA — Inter-University Computing Centre, Bologna, Italy;* [3]*SMR, Regional Meteorological Service of ARPA Emilia-Romagna and Atmospheric Dynamics Group, Department of Physics, University of Bologna, Italy*

ABSTRACT

Possible connections between spatial patterns, of limited regional extent and identified in teleconnection patterns and in blocking climatology studies, with hemispheric planetary-wave activity modes defined by the wave amplitude index (WAI) are investigated. The WAI probability density function (PDF) for the northern extratropics winter fields is estimated and the sensitivity of the WAI distribution to the presence of low-frequency variability modes is evaluated by stratifying the available dataset according to the sign of blocking and teleconnection indices. It is found that low-frequency variability modes affect both the mean and the variance of the wave amplitude index. Both the positive phase of the North Atlantic Oscillation (NAO) and the negative phase of the Pacific North American pattern (PNA) are associated with an enhanced frequency of very large amplitude planetary waves. Furthermore, distributions characterised by a maximum corresponding to high WAI values also exhibit a large variance. Negative NAO and positive PNA influence the mean and the variance of WAI PDF in the opposite sense. Similar results are found when the blocking index is considered. WAI PDFs relative to highly blocked months are broader with a secondary maximum corresponding to very high WAI values.

1. Introduction

Different observational and theoretical backgrounds motivated low-frequency variability studies since Rossby et al. (1939) classic paper on mid-latitude wave motion. More recently, a number of theoretical investigations and observational studies tend to support the idea of the existence of different weather regimes in the wintertime northern extratropical circulation (Charney and DeVore, 1979; Sutera, 1986).

The concept of weather regimes is based on the notion that the large-scale flow may evolve around various recurrent configurations. In other words,

the atmosphere is considered as a non-linear dynamical system with chaotic, but not totally random, behaviour oscillating between preferred zones of the atmospheric phase space ("flow regimes"). Although the idea of weather regimes is a long standing one (Namias, 1950; Rex, 1950b, Lorenz 1963), this notion was made more clear only in the last two decades. The existence of quasi-stationary regimes has also been investigated in modelling studies of the atmospheric global circulation (Reinhold and Pierrehumbert, 1982; Legras and Ghil, 1985; Haines and Hannachi, 1995). However, as far as the real atmosphere is concerned, flow regimes (in the wintertime circulation of the Northern Hemisphere) have been diagnosed principally on the basis of: (a) multimodality of the one-dimen-

* Corresponding author.
E-mail: paolina@bacino.geomin.unibo.it.

sional or multidimensional probability density function of circulation indices (Sutera 1986; Hansen and Sutera 1986; Molteni et al., 1988); (b) cluster analysis in an appropriate atmospheric phase space (Mo and Ghil, 1988; Molteni et al., 1990; Kimoto and Ghil, 1993; Cheng and Wallace, 1993); and (c) the existence of areas in phase space where the state vector is quasi-stationary (Vautard, 1990; Michelangeli et al., 1995).

A synthetic indicator of the amplitude of planetary waves (wave amplitude index, hereafter WAI) showing a bimodal density distribution was introduced by Sutera (1986). He found bimodality in the distribution of the amplitude of geopotential eddies at 500 hPa in the Northern extratropics after filtering the eddy fields in order to retain only zonal wavenumbers 2, 3 and 4. The two maxima in the WAI distribution were interpreted as two statistical flow regimes: the high and the low amplitude modes, respectively. Using a similar idea, Molteni et al. (1988) found a relationship between the observed bimodality in the planetary-scale wave amplitude and the variability of large-scale patterns. They showed that the distribution of the large-scale eddies of the 500 hPa geopotential height represented by the projection onto the linear space generated by the 1st five empirical orthogonal functions (EOFs), is bimodal. Moreover, the time coefficients associated with the amplitude of the 2nd EOF (characterised by a pattern dominated by a zonal wavenumber 3) and the 5th EOF (PNA-like, Wallace and Gutzler, 1981) also showed multimodality. The results of this study suggest that the high-amplitude mode is enhanced by more than one circulation-type regime, with different regimes showing opposite phases of the wavenumber-3 anomaly.

Cluster analyses of observational data have outlined a sketch of those structures in the atmospheric phase space corresponding to local probability density maxima, which can be identified as recurrent anomaly patterns. As expected, these anomalies are reminiscent of persistent and recursive patterns of the wintertime Northern Hemispheric flow (with transition time much shorter than residence time) as defined in well-known low-frequency variability observational works (Wallace and Gutzler, 1981; Dole, 1986; Yang and Reinhold, 1991). For example, Mo and Ghil (1988) and Molteni et al. (1990) indicate that spatial structures associated with cluster centroids

clearly project onto the PNA teleconnection pattern and the North Atlantic Oscillation (NAO, Hurrel, 1995).

However, although such regime patterns are associated with regional teleconnections, they also correspond more generally to quasi-stationary structures (persistent anomalies) of low-frequency variability, like for example blocking.

Historically, blocking is quoted as a classical example of large-scale recurrent weather pattern (Baur, 1951), but its classification as a global or local anomaly and an accepted theoretical interpretation explaining its dynamics are still problems of considerable interest and far from settled. In the global approach, blocked and zonal flows can be seen as multiple stationary equilibria as in Charney and De Vore (1979), or quasi-stationary states of the equation for the large-scale flow in which the Reynolds stresses due to small scales can lead to multimodality (Vautard and Legras, 1988). A number of studies examined the relation between the existence of multiple stationary solutions of highly truncated models, in particular solutions of the barotropic vorticity equation (Branstator and Opsteegh, 1989; Anderson, 1995), and the existence of multiple equilibria (Pierrehumbert and Malguzzi, 1984; Benzi et al., 1986, 1988). Different dynamical explanations of blocking based, for example, on the interactions between transient short-waves and low-frequency planetary waves (Green, 1977; Shutts, 1983; Malguzzi, 1993) have been proposed, providing strong support to the idea of regime-like behaviour (with rapid transitions between at least two, blocked and zonal, states). Moreover, in many observational studies (Dole and Gordon, 1983; Toth, 1992), it is suggested that baroclinic instability sets the timescales for the transition process between such regimes. This time scale is much shorter than the typical residence time scale (the latter of the order of weeks).

All these observational and modelling results of atmospheric low-frequency variability, weather regimes, blocking and planetary wave activity all come together to support the idea that different hemispheric large-scale regimes could contribute to the same global modes of atmospheric planetary wave activity as diagnosed by synthetic indices.

Within this framework, the main purpose of this paper is to study the possible connections between these regional extent patterns and the hemispheric planetary wave modes as defined in Sutera (1986).

In fact, it is well known that low-frequency variability modes, here identified either in blocking or in teleconnections, are characterised by their own "climate", which is different from the "true" climatology (i.e., the mean flow). On the other hand, an indicator of planetary wave amplitude like the WAI can be considered as the result of projecting daily maps observed in (multi-dimensional) physical space onto a mono-dimensional phase space. Thus, we want to study whether the behaviour of this indicator may reflect the different "climates" corresponding to different low-frequency variability regimes. The obvious link between atmospheric behaviour (recurrent and persistent patterns) and planetary waves in the physical space does not necessarily imply that the statistical proprieties of the atmosphere show different probability density maxima depending on wave amplitude and phase. In other words the WAI PDF corresponding to blocked/zonal planetary waves could apriori be similar to the climatological WAI PDF.

In order to assess whether the statistical properties of the WAI are sensitive to different circulation regimes, periods of time during which the atmosphere shows strong enough anomalies (of the type defined by the given regime) are selected and grouped. Then the WAI PDF for the northern extratropic winter fields is estimated and the sensitivity of the WAI distribution to such low-frequency variability modes is evaluated by stratifying the available dataset according to the sign of such indices (namely blocking and teleconnections). The resulting WAI PDFs are compared with the WAI PDF of the complete dataset (the climatological WAI PDF).

The paper is organised as follows. Section 2 gives a short description of the dataset used in this study. In Section 3, we define the blocking index and the low-frequency variability patterns considered and we discuss which version of these indicators we chose for each comparison. In Section 4, Sutera's planetary wave indicator (WAI) is described. Section 5 illustrates the comparison between WAI and regional low-frequency variability indices. In Section 6 global patterns are considered. Concluding remarks are to be found in Section 7.

2. Dataset

The observed dataset used in this study consists of daily 500 hPa geopotential height fields, for the

years 1949 through 1994. They were obtained by merging NMC analyses for the time period December 1949–December 1979 and ECMWF analyses for the subsequent period January 1980–February 1994. In such a way, a daily dataset of 44 entire years plus three months of an additional winter were made available. However, apart from the Wave Amplitude Index calculation, only winter (i.e., December, January and February) fields are considered in this study.

The original NMC data consist of Northern Hemisphere geopotential height fields on the NMC octagonal polar stereographic grid with a 381 km grid mesh, covering the whole Northern extratropics north of 20°N. ECMWF data are global fields represented by spherical harmonics coefficients truncated at triangular truncation 40. All the data were reinterpolated on a regular latitude–longitude grid (3.75 × 3.75) and only regions north of 22.5°N were considered.

3. Low-frequency variability modes

3.1. Blocking events

Atmospheric blocking contributes significantly to the low-frequency variability of the atmosphere. It has been one of the most intensely studied atmospheric phenomena since the early works of Rex (1950a, b). The difficulties involved in formulating a universally acceptable objective definition of a blocking event have led to the use of many different blocking criteria. Commonly used definitions include the occurrence of persistent positive height anomalies at particular locations (Dole and Gordon, 1983; Dole, 1978, 1986) or the occurrence of persistent anomalous midlatitude easterly flow (Lejenäs and Økland, 1983; Tibaldi and Molteni, 1990). More recently (Liu, 1994; Renwick and Wallace, 1996) a blocking index was calculated by projecting daily geopotential height anomaly fields on the synoptic patterns corresponding to sector (Pacific or Atlantic) blocking regimes.

This latter strategy, which is conceptually similar to the definition of Dole (1986), is the one used in this study, where the Tibaldi and Molteni (1990) (hereafter TM90) blocking criterion, based on the TM90 modification of the original index by Lejenäs and Økland (1983), is only used to define the (Atlantic and Pacific) spatial patterns

representing blocking onto which the anomaly fields are projected.

TM90 defined the frequency of blocking at a given longitude as the proportion of days in which (geostrophic) easterlies occur in a latitudinal band between 40°N and 60°N, while westerlies exceeding a given threshold are present North of 60°N. Here we use a 5 m/s threshold for the westerly flow, as suggested by Corti et al. (1997; the reader is referred to this paper for further details). Similarly to TM90, we identified two main regions of the Northern Hemisphere in which blocking events are more likely to occur: a Euro-Atlantic sector from 26.25°W to 41.25°E and a Pacific sector from 150°E to 138.75°W. Each sector exhibits a maximum blocking frequency at the "exit regions" of the two major Northern Hemisphere storm-tracks. A sector is taken to be blocked if three or more of its adjacent longitudes within its longitudinal limits are blocked. Moreover, following TM90, we have rejected blocking episodes of duration less than five days.

To obtain the synoptic patterns corresponding to sector blocking regimes, the following procedure has been applied. Data has been classified according to whether a day is zonal, Pacific blocked, or Atlantic blocked (including the 5-day minimum time duration requirement). Anomaly maps of the blocked regimes have been constructed by compositing (i.e., ensemble averaging) the maps of the two blocked categories and subtracting out the composite of all zonal days. Fig. 1 shows the 500-hPa mean maps of the anomalies corresponding to the two "winter blocking signatures". It can be noticed that blocking in both sectors is characterised by a neat and localised signature, with very little evidence of structures spatially remote from the quadrant under attention. Each one of these patterns can be considered, in its proper sector, a sort of "ideal blocking dipole". Therefore one can construct a blocking indicator as the measure of the resemblance between a given daily anomaly and the anomalies shown in Fig. 1.

A blocking index was computed by projecting the daily 500 hPa geopotential height anomaly field onto the patterns shown in Fig. 1, and transforming the resulting time series to have zero mean and unit variance. In this way two blocking indices, for the Euro-Atlantic and the Pacific sectors respectively, are obtained. Because of this
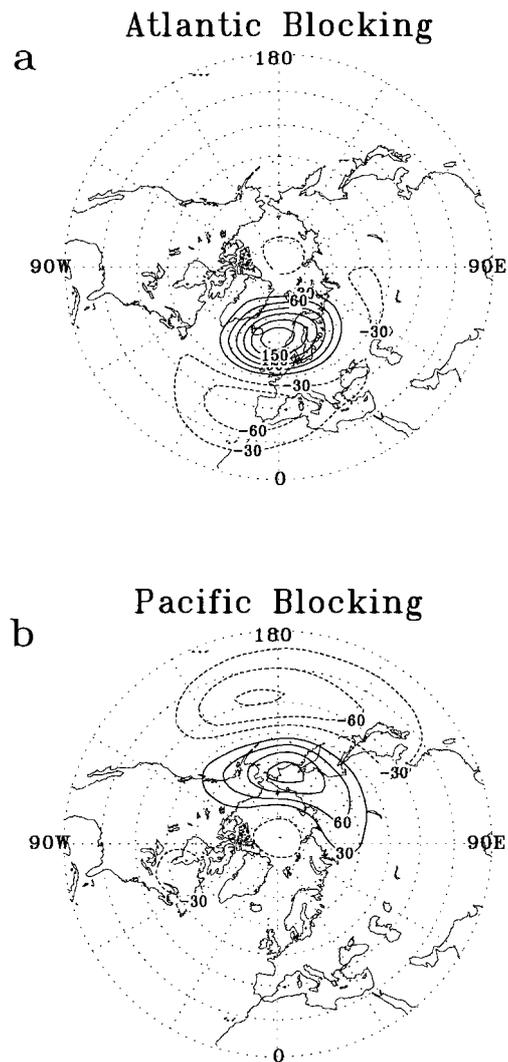

Fig. 1. "Blocking signature" (i.e., the difference of blocked and zonal days ensemble means) for the Euro-Atlantic (a) and Pacific (b) blocking in the December–February period. Contour interval 30m. Negative values are dashed.

definition, blocking indices in the two quadrants are completely independent. A large positive value of Euro-Atlantic/Pacific index corresponds to a blocked flow over the Euro-Atlantic/Pacific quadrant; on the contrary, a large negative value indicates a very zonal circulation type in that particular sector.

However, an instantaneous index such as this

is able to identify blocking-like structures but has to be supplemented by a further condition, reflecting the synoptic requirement of time duration, which distinguishes a transient blocking-like flow pattern from a true blocking event. Therefore we add the following condition: an Atlantic/Pacific *blocking day* is defined as a day with (Atlantic/Pacific) blocking index higher than a specified magnitude threshold M (here we choose $M = 0.5$); a Pacific/Atlantic *blocking event* is defined as a period of at least 5 consecutive blocked days. The same rule, but retaining daily indices $\leqslant -M$, is used to specify strong zonal days and events. Furthermore, by analogy with the regional blocking index, a "global" blocking index is defined requiring that both sectors are blocked at the same time (i.e., that both Atlantic and Pacific indices are $\geqslant M$).

The mean and the standard deviation of the number of blocked and zonal days (where only blocked/zonal days belonging to blocked events are considered) per month are reported in Table 1.

Our results are in substantial agreement with those found by Liu and Opsteegh (1995) and Corti et al. (1998). The Pacific sector is characterised by a larger month-to-month variability and a lower average number of blocked/zonal days. There are some cases when Pacific and Atlantic sectors behave, in terms of blocking, quasi-coherently. However, global blocking/zonal flow, as defined by our criterion, is an extremely rare event. On the other hand, the lack of correlation, in these two sectors was already pointed out by Lejenäs and Økland (1983), and as far as variability is concerned, our estimate of blocking variability, in the two sectors, unfortunately, cannot be compared to the work of Lejenäs (1995) because of the different time scales involved, monthly in our case, seasonal in the case of Lejenäs (1995).

Table 1. *Average number of blocking and zonal days per month*

	Atlantic sector	Pacific sector	Global
blocked days per month	9.5 ± 6.3	8.8 ± 7.7	0.9 ± 2.1
zonal days per month	9.8 ± 6.6	9.5 ± 8.2	0.9 ± 1.9

3.2. NAO and PNA

Fluctuations in the atmospheric winter flow, on seasonal time scales, appear to be dominated by a relatively small number of large-scale quasi-stationary modes of variability. In the Northern Hemisphere, the Pacific North American (PNA) pattern and the North Atlantic Oscillation (NAO) (Wallace and Gutzler, 1981; Barnston and Livezey, 1987) are examples of dominant patterns. Both are characterised by dipole structures straddling the "exit regions" of the climatological mean jet streams.

Two main approaches have been used in empirical studies to obtain these patterns of low frequency variability. The first, the so-called teleconnection method, is based on one-point correlation maps (Wallace and Gutzler, 1981). The second is that of rotated principal component analysis (RPCA) (Barnston and Livezey, 1987). In this work a third strategy has been adopted. In accordance with the mean winter location of NAO and PNA, two geographical sectors were specified. Relative to the NAO an Euro-Atlantic region, [22.5°N–90°N, 90°W–60°E], is considered whereas for the PNA we choose [22.5°N–90°N, 155°E–55°W]. Then, for each region, we performed a standard EOF analysis of time series of observed winter (DJF) anomalies of monthly averaged 500 hPa geopotential height.

The leading EOFs of Euro-Atlantic and American-Pacific sectors, scaled by the square root of their associated variance, are shown in Figs. 2a, b, respectively. The Euro-Atlantic EOF1 accounts for 28% of the total variance and provides a satisfactory representation of NAO. Over the American-Pacific sector, the leading EOF shows a typical PNA pattern and explains 31% of the total variance. Both of these patterns are computed as covariance between the 500 hPa geopotential height anomalies and the standardised principal components. In this way, the connections with anomalies located out of the boundaries of the specified sector can also be evaluated. It is interesting to note, for example, that the positive phase of Euro-Atlantic EOF1 (hereafter NAO) is related to a positive anomaly centred over Pacific and North-East Asia, while the American-Pacific EOF1 (hereafter PNA) anomaly is accompanied by two weak anomalies of opposite sign over

Euro−Atlantic EOF1
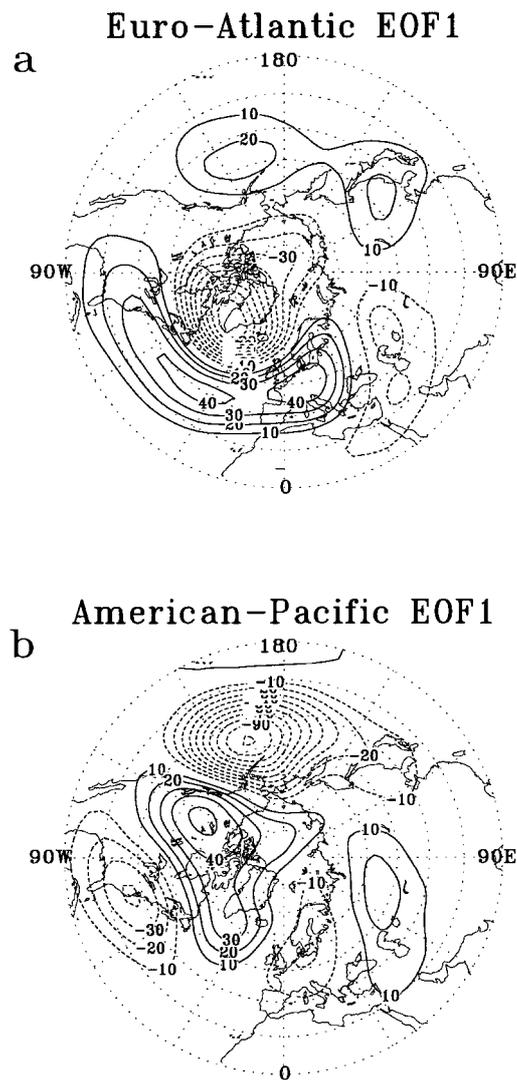
a

American−Pacific EOF1

b

Fig. 2. (a) First 500 hPa geopotential height Euro-Atlantic EOF (monthly anomalies) for winter (DJF) from NMC analysis data. (b) as in (a) but for the first American-Pacific EOF. Contour interval 10m. Negative values are dashed.

central Asia (positive) and Western-North Europe (negative).

The time series of the standardised principal components associated with the leading EOFs of Euro-Atlantic and American-Pacific sectors (hereafter considered as NAO and PNA winter months indices respectively) are shown, as open circles, in Figs. 3a, b respectively. It is worth noting the

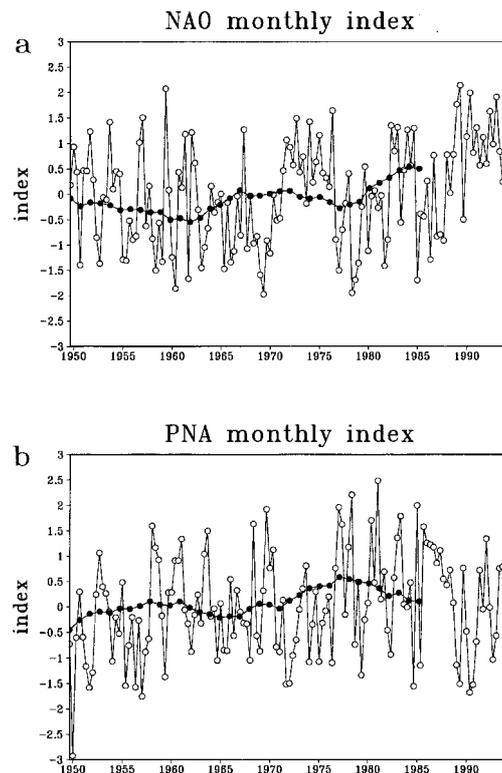### NAO monthly index

a

PNA monthly index

b

Fig. 3. Time series of the principal components of the two dominant empirical orthogonal functions of 500-hPa monthly-mean observed geopotential height over the northern hemisphere for the period 1949–1994. (a) Euro-Atlantic sector; (b) American-Pacific sector. Open circles: monthly time series; solid circles: 10-year running means of the monthly series.

presence of a clear positive trend (highlighted by the superimposed 10-year running mean, solid circles) in the values of the NAO index during the last twenty years, which has been reported by various authors (Hurrel, 1996; Hurrel and Van Loon, 1997; Zorita and Frankignoul, 1997). A corresponding, but weaker, trend can be observed in the time series of the PNA index. However, on monthly time scales the (negative) non-negligible correlation between the NAO and the PNA indices (−42%) suggests a sort of "hemispheric coherence" in the atmospheric circulation, i.e., there appear to be occasions when regional regimes over Pacific and Atlantic behave as partially anti-synchronised (chaotic) oscillators (Palmer, 1999).

4. Wave amplitude index

The rationale behind the definition and construction of the wave amplitude index, introduced by Sutera (1986), results primarily from the theoretical works of Charney and DeVore (1979) and Wiin-Nielsen (1979) on simple, barotropic, low-order models of midlatitude planetary wave/mean flow interaction. They found multiple steady equilibria due to the presence of an instability associated to the topographically resonant flow. In particular they found, for certain values of model parameters, two stable solutions characterised respectively by "high" and "low" wave amplitude. Many authors viewed these two stable equilibria as idealisations of "zonal" and "blocked" states of the real atmosphere and supported the idea of a midlatitude winter atmosphere "fluctuating" between different flow regimes.

To assess the existence of such low-frequency multiple flow regimes in the middle latitudes of the winter hemisphere, Sutera (1986) constructed the wave amplitude index (WAI) as a combination of the amplitudes of the first few planetary waves most susceptible to undergo resonance with the lower boundary condition. In this study we use this index as a measure of the extratropical large scale circulation on a hemispheric coverage.

Following Sutera's description, the WAI is calculated as follows. Each daily map of the observed 500 hPa geopotential height, $Z(\lambda, \phi, t)$, is meridionally averaged over the midlatitude band $[45°-70°N]$ chosen according to Hansen and Sutera (1986, hereafter HS86). The obtained field $Z(\lambda, t)$ is then Fourier decomposed and zonal wavenumbers 2 to 4 retained. Finally, the WAI is defined as the root-mean square value of the sum of squares of the retained wavenumbers:

$$\text{WAI} = \left(\sum_{i=2}^{4} |2\bar{Z}_i(t)^2| \right)^{1/2} \tag{1}$$

The effect of the averaging procedure is to remove or weaken the contribution to the index from planetary waves with complicated meridional structure and principally select waves with broad latitudinal extent. Furthermore, a 5-day low pass filter is applied to the WAI time series. To remove the annual cycle and its subharmonics, the same procedure used in HS86 has been applied: the time series has been Fourier transformed, then resynthesized after removal of periods ranging from 22 to 9 months. The final result of this analysis is a time series representing the time behaviour of the planetary wave amplitude through the 44 years (plus one additional winter) considered. Since our study is devoted to the winter season, we shall focus hereafter only on the index time series during December, January and February.

The probability density function of the WAI anomaly, computed using a Gaussian kernel estimator (Marshall and Molteni, 1993), is shown in Fig. 4a. This distribution exhibits two local maxima (M1 and M2) with amplitudes lower and higher than normal respectively and a third local maximum (M3) with very high planetary wave amplitude. The first two maxima are essentially to those found by HS86 from 15 winters (1964/65 through 1979/80) and more recently confirmed by the same authors (Hansen and Sutera, 1995) on a larger dataset. Their statistical significance has been proved in HS95 by means of Monte Carlo tests. The 3rd maximum belongs to the distribution tail and is poorly populated.

To observe the mean anomalies corresponding to high and low WAI values, HS86 have constructed composites of hemispheric geopotential height fields resulting from the partitioning of the PDF into low (mode 1) and high (mode 2) amplitude modes. In particular, they defined "mode 1" and "mode 2" by compositing daily fields with WAI anomaly values respectively lower and higher than the distribution minimum. Using this definition, we computed the two modes from our dataset and the associated height anomalies are displayed in Figs. 4b, c. These patterns compare very well with those of HS86. As expected, the low-amplitude mode (Fig. 4b) is associated with a fairly zonal flow, while the high-amplitude mode (Fig. 4c) corresponds to an amplified planetary wave pattern. The two maps are dominated by anomalies of substantial amplitude at planetary-scale wavelengths, particularly wavenumber 2. In both cases the whole pattern is of hemispheric extent, but the anomalies are larger over the Pacific North American sector.

Temporal changes between low and high WAI values are quite rapid, while the residence time in a given WAI "mode" is comparatively longer. Considering the entire 45-winter time series, the total time over which a transition occurs (tran-

WAI – winters 49/50 – 93/94

a

Mode 1 winter anomaly   ## Mode 2 winter anomaly

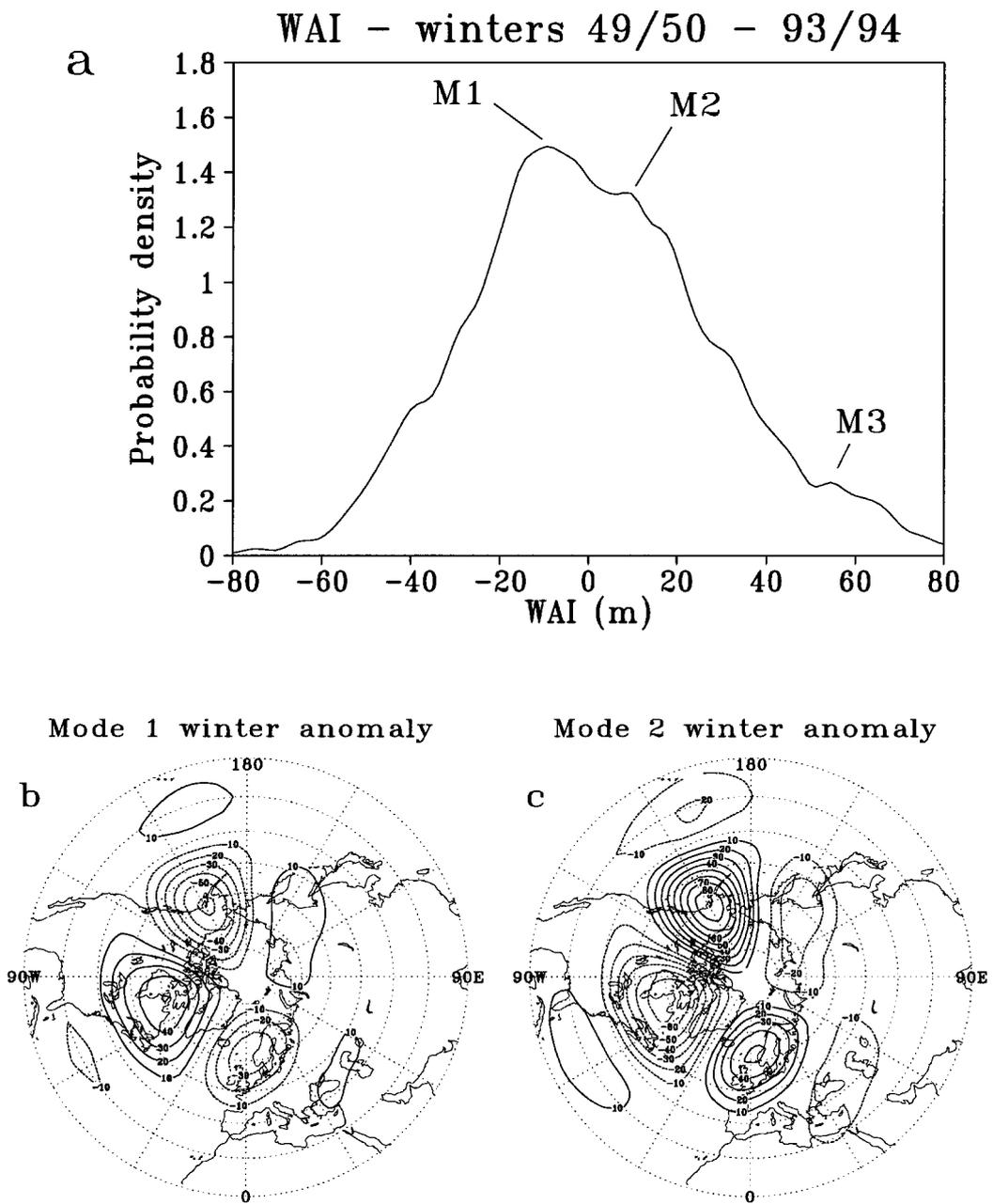b   c

Fig. 4. (a) Probability density estimation of the WAI computed in the [45°N-70°N] zone from the winters 1949–1994. (b) and (c) Mode 1 and Mode 2 composites (see text). Contour interval 10m. Negative values are dashed.

sitions have been defined in agreement with Hansen, 1988) is, on average, 4 days, while the duration of events of either mode is about 10 days.

5. Wave amplitude index and low-frequency variability modes

In this section, we investigate the relationship between those patterns of limited regional extent like blocking and teleconnections, as defined by the above indices, and the hemispheric planetary wave activity modes defined by the wave amplitude index. More precisely, the question we address here is whether and how the statistical properties of the wave amplitude index are "sensitive" to different circulation regimes. In order to obtain homogeneous results from a statistical (and graphical) point of view, the following common methodology has been applied.

5.1. Tools and methodology

To investigate the sensitivity of the planetary wave amplitude index to low-frequency variability modes, we start by classifying the (135) winter months of our dataset according to the sign of blocking and teleconnections.

The classification of NAO and PNA months is made stratifying the Euro-Atlantic and Pacific EOF1 principal components shown in Fig. 3. As far as blocking events are concerned, the stratification criterion is made on the basis of the number of blocked/zonal days (belonging to a blocking/zonal event as defined in Subsection 3.1) per month. There is something arbitrary about using a monthly indicator, because the time scale of the evolution of blocking is mostly shorter than one month. However it is an observational fact that the mean flow of a blocked/zonal month is different from the climatology itself. On the other hand, as discussed in the introduction, to assess whether these differences in the mean flow affect the statistical behaviour of the WAI, is exactly the scope of this study.

After transforming the WAI time series to have zero mean and unit variance, we compare, for each low-frequency index, the WAI PDF of the whole sample with those obtained from the classified samples. The resulting PDFs are shown in Figs. 5, 6. Means and standard deviations of the distributions are listed in Tables 1, 2.

Fig. 5 shows 5 examples of WAI PDFs stratified according to Atlantic blocking (panels a, b), Pacific blocking (panels c, d) and Global blocking (panel e) indices, respectively. WAI PDFs stratified according to teleconnection indices are shown in Fig. 6 (Fig. 6a, b: NAO; Fig. 6c, d: PNA; Fig. 6e: NAO/PNA global mode). In all cases, the control (climatological) distribution (i.e., the PDF of the whole dataset) is shown as a solid line. The dashed and dotted curves refer to periods of extremely positive and negative indices, respectively. The upper panels of Figs. 5, 6 show the WAI distributions during the first 12 stratified months (i.e., the 12 winter months in which the relevant low-frequency index exhibits the most extreme positive/negative values). Middle panels are relative to 6-month samples. They are subsets of the former 12 months and consist of the most extreme events. Finally, the lower panel shows, in both figures, the WAI distributions of the 6-month samples classified by the global version of blocking index (Fig. 5e) and teleconnection index (Fig. 6e), respectively.

All the PDFs have been generated using a Gaussian kernel estimator (Silverman 1986; see also Marshall and Molteni 1993 for more details in a similar application). The control WAI PDF (shown here for reference as a solid line) is virtually that shown in Fig. 4a, except for the smoothing. In fact the smoothing (here the same for all the distributions considered) is such that the probability of obtaining a multimodal estimate from a (a priori known) unimodal distribution is lower than 10% when applied to 12 or 6-month samples.

5.2. WAI versus blocking index

Figs. 5a–d shows the WAI PDFs stratified according to the sign of Atlantic (a, b) and Pacific (c, d) blocking indices respectively. Means and standard deviations of the WAI index for different flow regimes are listed in Table 2. The results shown in both figures and table indicate that the WAI PDFs relative to very blocked months are broader with a secondary maximum corresponding to very high WAI values (in both sectors, more pronounced during Pacific blocked months). An enhanced variability of WAI is found when the Pacific sector is blocked. The opposite is true for low values of blocking indices ("zonal" months).

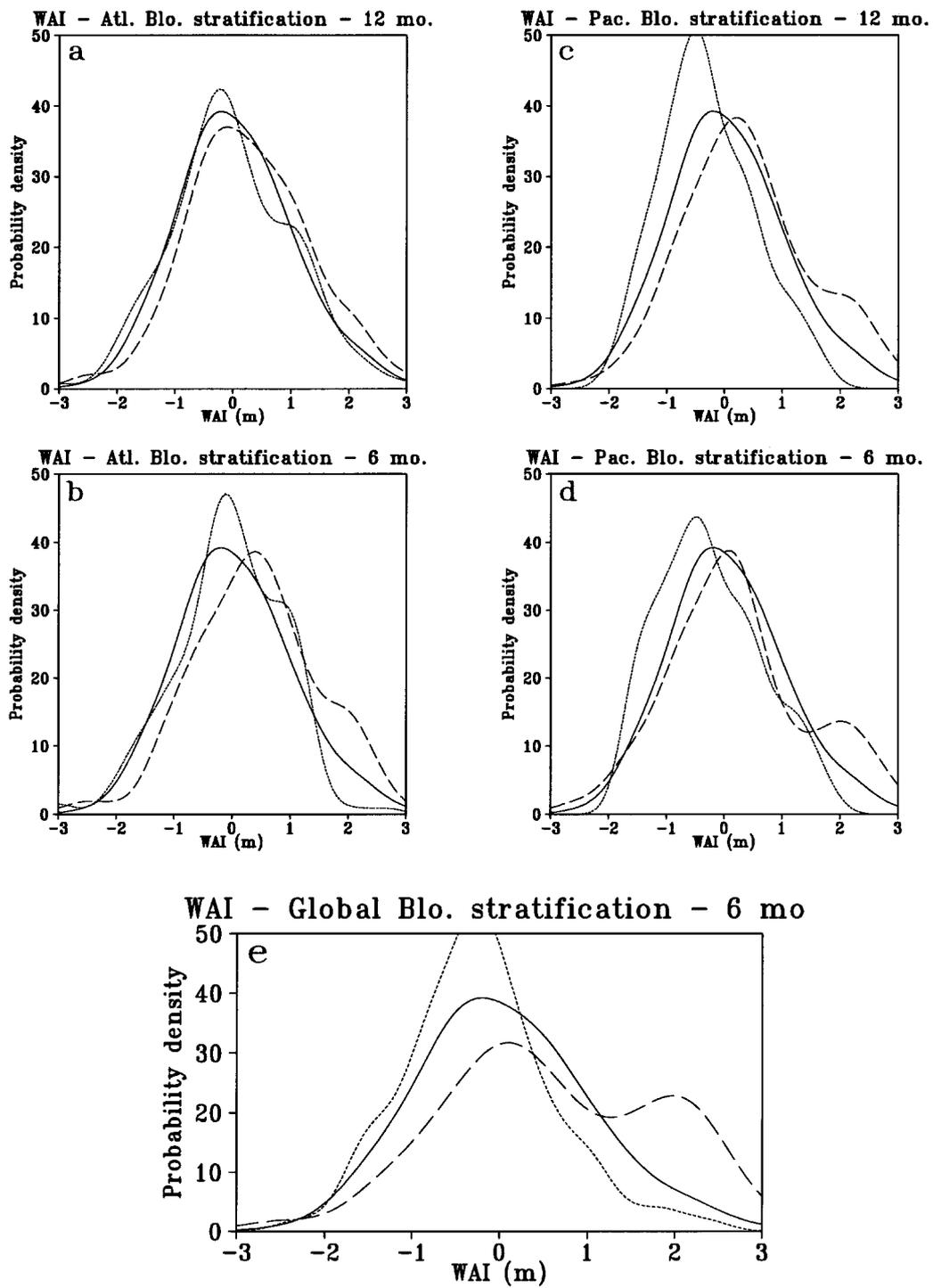The results, in terms of PDFs, of the stratifica-

WAI − Atl. Blo. stratification − 12 mo.

WAI − Pac. Blo. stratification − 12 mo.

WAI − Atl. Blo. stratification − 6 mo.

WAI − Pac. Blo. stratification − 6 mo.

WAI − Global Blo. stratification − 6 mo

Table 2. *Mean and standard deviation of the WAI PDFs shown in Fig. 5*

Control	Mean ± std 0.00 ± 1.00	
	12 months mean ± std	6 months mean ± std
Atlantic blocking (Figs 5a, b, dashed line)	0.41 ± 1.07	0.42 ± 1.15
Atlantic zonal flow (Figs 5a, b, dotted line)	0.2 ± 1.0	0.12 ± 1.07
Pacific blocking (Figs 5c, d, dashed line)	0.30 ± 1.20	0.21 ± 1.21
Pacific zonal flow (Figs 5c, d, dotted line)	−0.27 ± 0.87	−0.25 ± 0.88
global blocking (Fig. 5e, dashed line)	—	0.60 ± 1.24
global zonal flow (Fig. 5e, dotted line)	—	−0.23 ± 0.84

tion relative to global blocking are shown in Fig.5e. The variance of WAI is enhanced for large values of the index with a shift of the mean towards positive values (Table 2). The blocked distribution is clearly bimodal and both maxima correspond to high planetary wave amplitudes.

5.3. WAI versus PNA/NAO patterns

If we now consider the distributions of WAI with stratification according to the teleconnection patterns (Fig. 6), we note that the sign of the NAO/PNA indices does indeed influence the WAI PDF. A preponderantly negative PNA phase corresponds to an enhanced probability of high amplitude planetary waves. To the contrary, negative NAO is a favourable condition for a more zonal flow. However, differences between the effects of positive PNA and negative NAO are not as simple. In fact, the variance of WAI is reduced when the phase of NAO/PNA is negative/positive, while it is enhanced when these phases are reversed (Table 3). These features are present in all the examples considered, but they more clearly stand

out when the 6-month extreme events samples are considered. In such cases, the WAI distributions also exhibit two maxima. The first is a "climatological" maximum positioned around the distribution mean; the second maximum may correspond to either high or low planetary wave amplitudes depending on the sign of NAO/PNA stratification. It is positive when negative PNA or positive NAO are considered; and negative otherwise.

These results indicate that the phases of the NAO and the PNA can affect in some way the amplitude of the planetary waves as measured by Sutera's WAI. On the other hand, even though PNA and NAO patterns can fluctuate independently for much of the time (Wallace, 1996), and therefore could be considered as independent regional patterns, the relatively large negative correlation (−0.42) between the two time series indicates that there are occasions when such regional regimes over the Pacific and Atlantic do vary coherently. In such cases, characterised by a sort of PNA–NAO global mode, an even stronger influence on the wave amplitude index distribution should be expected. In particular, during periods characterised by positive PNA and negative NAO we can observe a sharper WAI distribution with enhanced probability of low amplitude planetary waves. On the contrary, the negative PNA and positive NAO phases correspond to an increased variability in the amplitude of planetary waves and also to an increased frequency of very high amplitude waves.

The lower panel in Fig. 6 shows the 6-month sample of WAI PDFs stratified according to the sign of an index of such a (kind of) coupled PNA–NAO "global" mode. Because of the negative correlation between the two patterns, this new index was constructed by taking the difference between the two PNA and NAO indices. Fig. 6 shows that the condition of positive PNA/negative NAO is indeed a favourable one for high amplitude waves, while the opposite phase is related to a more zonal flow. Both distributions exhibit also two well separated maxima.

Fig. 5. WAI probability density functions, stratified by the sign of blocking index. (a) 12-month samples having the largest (positive and negative) values of the Atlantic blocking index; (b) as (a) but for 6-month samples; (c) 12-month samples having the largest (positive and negative) values of the Pacific blocking index; (d) as (c) but for 6-month periods; (e) 6-month samples having the largest (positive and negative) values of the Global blocking index. Solid line: control climate; dashed line: positive values; dotted line: negative values.
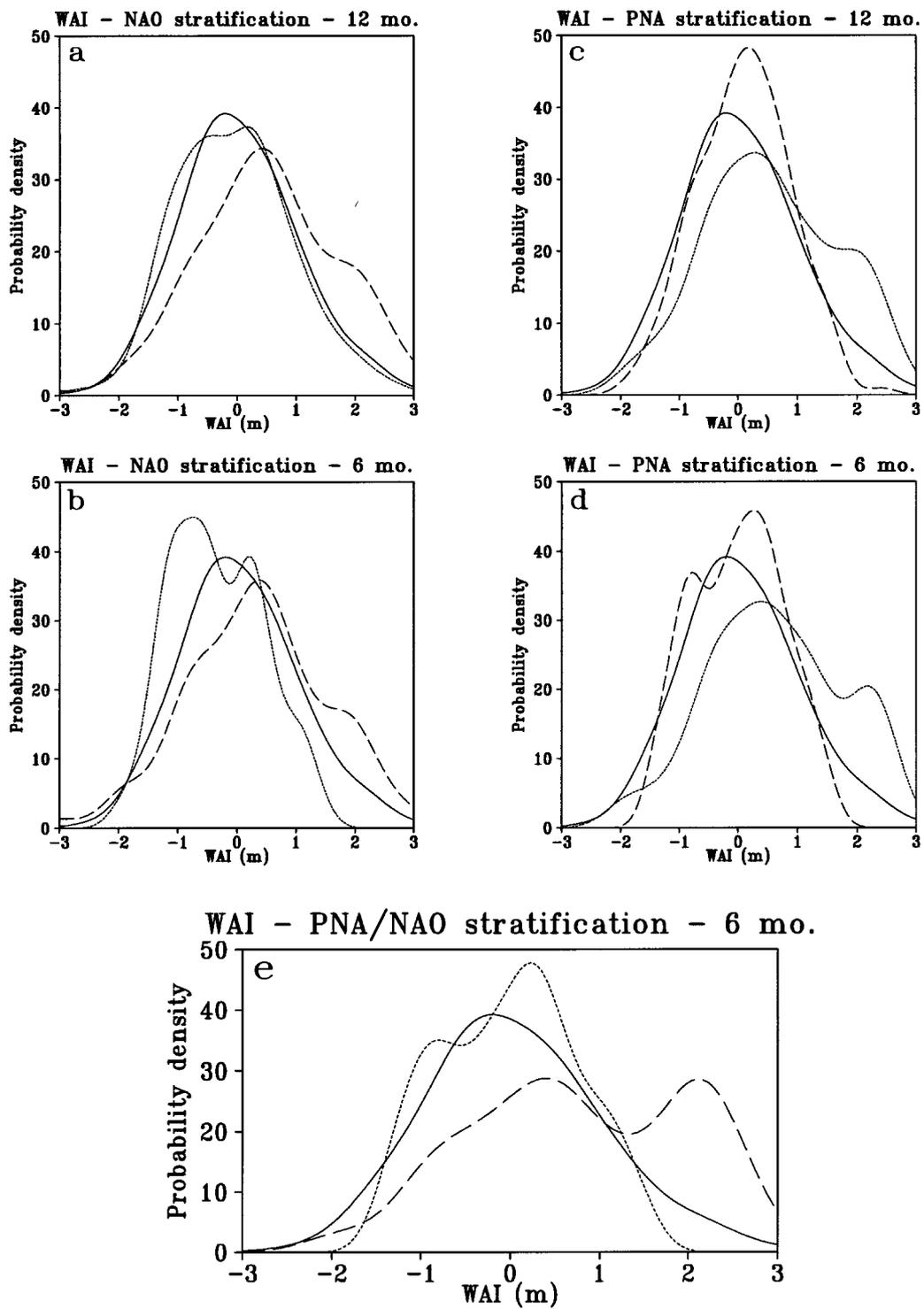
WAI − NAO stratification − 12 mo.

WAI − PNA stratification − 12 mo.

WAI − NAO stratification − 6 mo.

WAI − PNA stratification − 6 mo.

WAI − PNA/NAO stratification − 6 mo.

Table 3. *Mean and standard deviation of the WAI PDFs shown in Fig. 6*

Control	Mean ± std 0.00 ± 1.00	
	12 months mean ± std	6 months mean ± std
Pos. NAO (Figs 6a, b, dashed line)	0.53 ± 1.18	0.33 ± 1.17
Neg. NAO (Figs 6a, b, dotted line)	−0.04 ± 0.97	−0.33 ± 0.78
Pos. PNA (Figs 6c, d, dashed line)	0.08 ± 0.79	−0.01 ± 0.76
Neg. PNA (Figs 6c, d, dotted line)	0.55 ± 1.11	0.62 ± 1.13
Pos. PNA Neg. NAO (Fig. 6e, dashed line)	—	−0.01 ± 0.76
Neg. PNA Pos. NAO (Fig. 6e, dotted line)	—	0.79 ± 1.22

6. The PNA–NAO global mode

In order to test this hypothesis of a "global" PNA–NAO mode, an Empirical Orthogonal Function analysis was applied to the hemispheric domain monthly data. The spatial patterns of the two leading EOFs are shown in Fig. 7. They are very similar to those found by Kimoto and Ghil (1993). The height anomaly associated with EOF1 projects both onto the negative PNA and the positive NAO explaining the 18.3% of the total variance. The second EOF (12% of the variance) exhibits a good resemblance with the 500 hPa geopotential height manifestation of the so-called "Cold Ocean Warm Land" pattern, which, to a first approximation, describes recent climate change in surface temperature on the decadal time scale (Wallace et al., 1995). Furthermore the spatial structure of both EOFs is very similar to that of well documented weather regimes (clusters in phase space). These patterns correspond very clearly with the so-called cluster-5 centroid (EOF1) and cluster-2 centroid (EOF2) found by Molteni et al. (1990), and based on 5-day mean 500 hPa geopotential height fields. They also agree
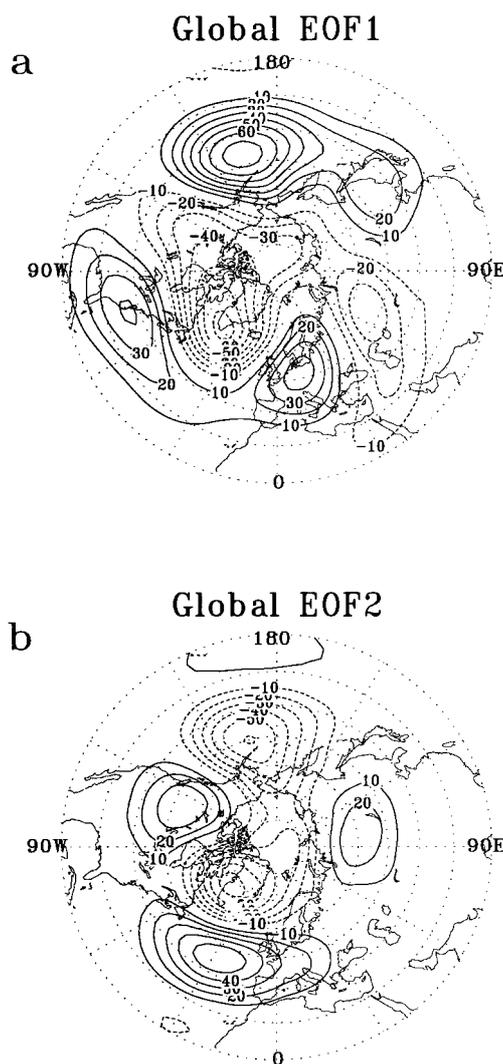
Global EOF1

Global EOF2

Fig. 7. (a) First 500 hPa geopotential EOF monthly anomaly during winter (DJF) from NMC analysis data. (b) As in (a) but for the second EOF. Contour interval 10m. Negative values are dashed.

well with centroids found using different cluster-analysis methods (Mo and Ghil, 1988; Kimoto and Ghil, 1993).

Fig. 8 shows the WAI PDFs stratified according

Fig. 6. As in Fig. 5 but the WAI PDFs are stratified by the sign of NAO/PNA indices. (a) 12-month samples stratified by NAO; (b) 6-month samples stratified by NAO; (c) 12-month samples stratified by PNA; (d) 6-month samples stratified by PNA; (e) 6-month samples stratified by the PNA–NAO global index. Solid line: control climate; dashed line: positive values; dotted line: negative values.
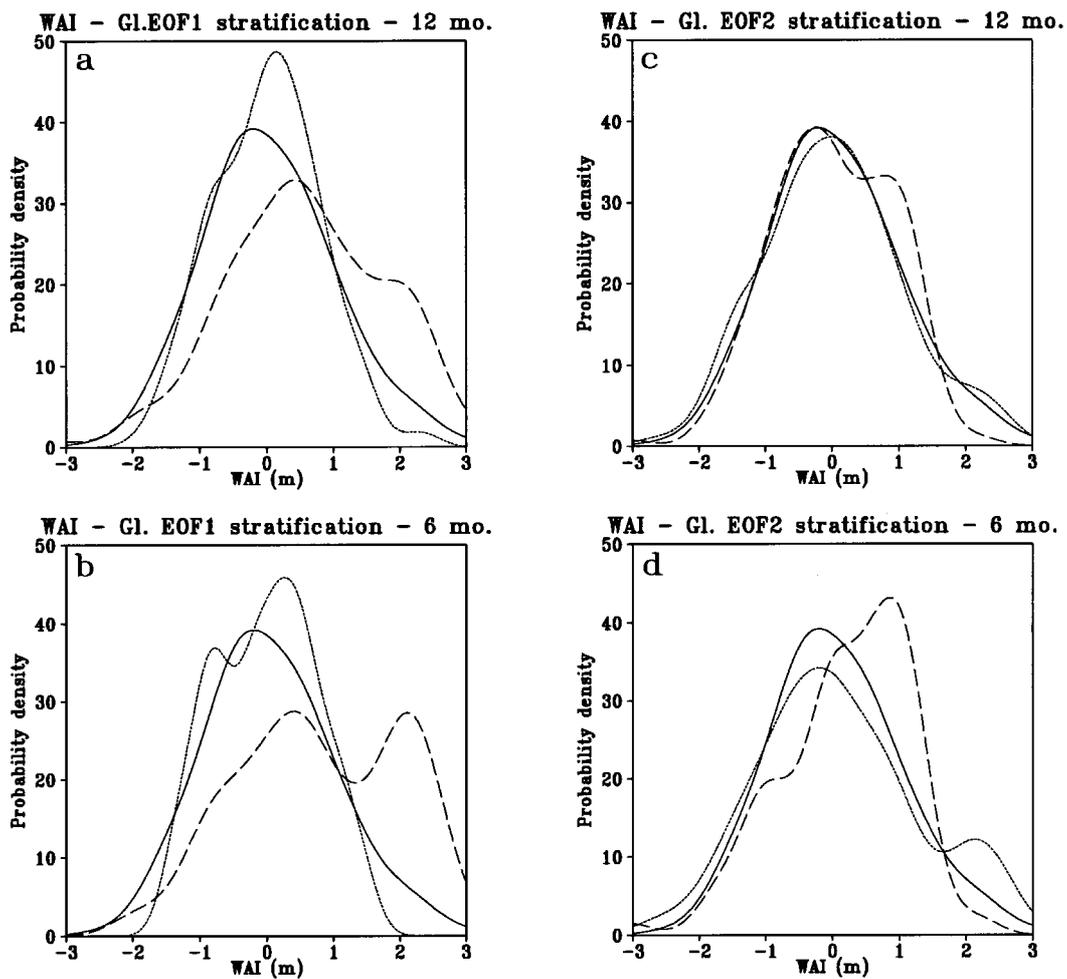
Fig. 8. WAI probability density functions, stratified by the sign of global EOF1 and EOF2. (a) 12-month samples having the highest (positive and negative) values of the EOF1 index; (b) as (a) but for 6-month samples; (c) 12-month samples having the highest (positive and negative) values of the EOF2 index; (d) as (c) but for 6-month samples. Solid line: control climate; dashed line: positive values; dotted line: negative values.

to the sign of global EOF1 and EOF2. It is confirmed that the positive phase of EOF1 (i.e., the negative PNA/positive NAO mode) is indeed a favourable condition for high amplitude waves, while the negative phase is related to a more zonal flow. EOF2 influences the statistics of WAI as well. The probability of having high amplitude planetary waves is enhanced when EOF2 is positive.

Considering together Figs. 7, 8, the following remarks can be made. The fact that both EOFs,

which are strongly reminiscent of two low-frequency variability regimes (clusters), are of hemispheric extent, confirms the existence of a degree of hemispheric coherence between the circulation anomalies. On the other hand, WAI distributions associated with the opposite phases of both global EOFs (at least in the case of more extreme events) exhibit two well defined maxima. For example, during positive EOF1 periods (dashed line in Fig. 8b) the WAI fluctuates between climatological and very high wave amplitude states; whilst

negative EOF1 periods (dotted line in Fig. 8b) are characterised by the same climatological maximum and a further secondary maximum corresponding to very low amplitude waves. This result seems to indicate that, within the "climate" of a given low-frequency variability regime, one may have (in turn) two regimes characterised by high and low amplitude planetary waves, respectively.

7. Discussion and conclusions

In this paper, we have addressed the problem of the possible relationships between regional and global indices of low-frequency variability and the (global) indicator of planetary wave amplitude suggested by Sutera (1986).

First we have evaluated the observed indices in physical space; then we have calculated WAI PDFs for the northern extratropic winter fields by stratifying the available dataset according to the sign of such indices (namely blocking and teleconnections) and comparing the resulting WAI PDFs with the WAI PDF of the complete dataset. This stratification has been done using extreme events of low-frequency variability in order to see whether and how the specific "climate" of these events is reflected by the statistical properties of the WAI index. It was found that low-frequency variability modes affect both the mean and the variance of the wave amplitude index probability density functions.

As far as blocking indices are concerned, we confirmed the result of Lejenäs and Økland, 1983 that Pacific and Atlantic sector are not particularly correlated in this respect. However, periods with a prevalent "regional blocked flow" (Pacific or Atlantic) are in general characterised by higher values of the (hemispheric in nature) wave amplitude index. These results are to be expected and can be understood by simply noting that large amplitude ridges of quasi-stationary planetary-scale waves (with the correct phase) are generally needed to construct a blocking high. Furthermore, a number of observational studies showed that blocking is in general associated with an enhancement of the amplitude of stationary waves (Tung and Lindzen, 1979; Austin, 1980; Hansen and Sutera, 1993). It could perhaps be more interesting to note that WAI PDFs relative to prevailing

blocked flow in the Pacific sector show an increased variance. One could argue that this could be a (trivial) consequence of the monthly-averaged blocking index. Since the time scale typical of blocking lifetime is somewhat shorter than a month, blocked-months-on-average may show a larger variability of the planetary waves simply due to the onset and decay of one or more blocking events during the month. However, the fact that the enhanced variability concerns especially the Pacific region (together with the fact that one-month long blocks are not so uncommon), suggests that, at least for this region, blocked flow is particularly related to an enhanced planetary wave activity.

Turning to the possible relationships between regional teleconnections and wave amplitude index, the first thing to note is that positive NAO and negative PNA are confirmed to present some evidence of spatial coherence on monthly time scales. In practice, although Pacific and Atlantic sectors regimes variabilities are normally quasi independent, they become partially synchronised from time to time. The correlation found (42%) is not particularly high, but it should be noted that a linear correlation analysis may not be an appropriate way to study a possible "partial synchronisation" since the phenomenon, certainly, involves nonlinear atmospheric chaotic synchronisation as discussed by Duane (1997) in the (more general) context of interhemispheric synchronisation, which goes well beyond the scope of this work. Furthermore, the positive phase of NAO and the negative phase of PNA are both associated with an enhanced frequency of very high amplitude planetary waves. Distributions characterised by a maximum corresponding to high WAI exhibit also large variance, while negative NAO and positive PNA influence the mean and the variance of WAI PDF in the opposite sense. These features are particularly clear when WAI distributions of the 6-month sample stratified by the PNA–NAO global index are considered (extreme events). In such case, both WAI distributions exhibit two well separated maxima.

In order to test the above somewhat speculative conclusions on the relations between PNA and NAO patterns and the high amplitude planetary-scale regime as perceived by the WAI index, we performed a hemispheric EOF analysis and stratified the WAI index according to it. We found

results very similar to those described by the global PNA–NAO index constructed with separate (regional) PNA and NAO indices, recovering at the same time hemispheric spatial structures of low-frequency time-variability previously found in well-accepted weather regimes studies.

These observations suggest some further speculations about possible global regimes. The larger wave amplitude mode present in many stratified WAI PDFs (corresponding mostly to extreme cases) identifies with what Hansen and Sutera (1995) call the "amplified wave regime". This regime seems to be particularly related to what we have called a hemispheric-scale PNA–NAO global mode, possibly due to the mostly constructive phase relation between PNA and NAO taking place in this case. On the other hand, a number of flow regimes studies based on cluster analysis have identified a global pattern which bears a close resemblance to this amplified wave regime. For instance, cluster 2 of Mo and Ghil (Mo and Ghil, 1988) and cluster 5 of Molteni et al. (Molteni et al., 1990) are examples of such pattern. More recently, Cheng and Wallace (1993) and Corti et al. (1999) identified clusters (i.e., Cheng and Wallace "A" cluster and Corti et al. "B" cluster) reminiscent of the amplified wave regime.

8. Acknowledgements

REFERENCES

Anderson, J. L. 1995. A simulation of atmospheric blocking with a forced barotropic model. *J. Atmos. Sci.* **52**, 2593–2608.

Austin, J. F. 1980. The blocking of middle latitude westerly winds by planetary waves. *Q. J. R. Meteorol. Soc.* **106**, 327–350.

Barnston, A. G. and Livezey, R. E. 1987. Classification, seasonality and persistence of low-frequency atmospheric circulation patterns. *Mon. Weather Rev.* **115**, 1083–1126.

Baur, F. 1951. Extended range weather forecasting. In: *Compendium of Meteorology*, American Meteorological Society, 814–833.

Benzi, R., Malguzzi, P., Speranza, A. and Sutera, A. 1986. The statistical proprieties of general atmospheric circulation: Observational evidence and minimal theory of bimodality. *Q. J. R. Meteorol. Soc.* **112**, 661–674.

Benzi, R., Iarlori, S., Lippolis, G. and Sutera, A. 1988. Steady non-linear response of a barotropic quasi-unidimensional model to complex topography. *J. Atmos. Sci.* **45**, 3313–3319.

Branstator, G. and Opsteegh, J.D. 1989. Free solutions of the barotropic vorticity equation. *J. Atmos. Sci.* **46**, 1799–1814.

Charney, J. G. and De Vore, J. G. 1979. Multiple flow equilibria in the atmosphere and blocking. *J. Atmos. Sci.* **36**, 1205–1216.

Cheng, X. and Wallace, J. M. 1993. Cluster analysis on the Northern Hemisphere wintertime 500-hPa height field: Spatial patterns. *J. Atmos. Sci.* **50**, 2674–2695.

Corti, S., Giannini, A., Tibaldi, S. and Molteni, F. 1997. Patterns of low-frequency variability in a three-level quasi-geostrophic model. *Clim. Dyn.* **13**, 883–904.

Corti, S., Molteni, F., and Palmer T. N., 1999. Signature of recent climate change in frequencies of natural atmospheric circulation regimes. *Nature*, **398**, 799–802.

Dole, R. M. 1978. The objective representation of blocking patterns. In *The general circulation: theory, modelling and observations*. Notes from a Colloquium, Summer, 1978. NCAR/CQ-6 + 1978 — ASP, 406–426.

Dole, R. M. 1986. Persistent anomalies of the extratropical northern hemisphere wintertime circulation: structure. *Mon. Weather Rev.* **114**, 178–207.

Dole, R. M. and Gordon, N. D. 1983. Persistent anomalies of the Northern Hemisphere wintertime circulation. Geographical distribution and regional persistence characteristics. *Mon. Weather Rev.* **106**, 746–751.

Duane, G. S. 1997. Synchronised chaos in extended systems and meteorological teleconnections. *Phys. Rev. E* **56**, 6475–6493.

Green, J. S. A. 1977. The weather during July 1977: some dynamical considerations of the drought. *Weather* **32**, 120–128.

Haines, K. and Hannachi A. 1995. Weather regimes in the Pacific from a GCM. *J. Atmos. Sci.* **52**, 2444–2462.

Hansen, A. R. 1988. Further observational characteristics of bimodal planetary waves: Mean structure and transitions. *Mon. Weather Rev.* **116**, 386–400.

Hansen, A. R. and Sutera, A. 1986. On the probability density distribution of large-scale atmospheric wave amplitude. *J. Atmos. Sci.* **43**, 3250–3265.

Hansen, A. R. and Sutera, A. 1993. A comparison between planetary-wave flow regimes and blocking. *Tellus* **45A**, 281–288.

Hansen, A. R. and Sutera, A. 1995. The probability density distribution of the planetary-scale atmospheric wave amplitude revisited. *J. Atmos. Sci.* **52**, 2463–2471.

Hurrel, J. W. 1995. Decadal trends in the North Atlantic

Oscillation: Regional temperature and precipitation. *Science* **269**, 676–679.

Hurrel, J. W. 1996. Influence of variations in extratropical wintertime teleconnections on Northern Hemisphere temperatures. *Geophys. Res. Lett.* **23**, 665–668.

Hurrel, J. W. and Van Loon, H. 1997. Decadal variations in climate associated with the North Atlantic oscillation. In: *Climate change. Proc. Int. Workshop on Climatic change at high elevation sites*, Wengen, Switzerland.

Kimoto, M. and Ghil, M. 1993. Multiple flow regimes in the Northern Hemisphere winter. Part I: Methodology and hemispheric regimes. *J. Atmos. Sci.* **50**, 2645–2673.

Legras, B. and Ghil, M. 1985. Persistent anomalies, blocking and variations in atmospheric predictability. *J. Atmos. Sci.* **42**, 433–471.

Lejenäs, H. and Økland, H. 1983. Characteristic of northern hemisphere blocking as determinated from a long time series of observational data. *Tellus* **35A**, 350–362.

Lejenäs, H. 1995. Long term variations of atmospheric blocking in the Northern Hemisphere. *J. Met. Soc. Japan* **73**, 79–89.

Liu, Q. 1994. On the definition and persistence of blocking. *Tellus* **46A**, 286–298.

Liu, Q. and Opsteegh, T. 1995. Interannual and decadal variations of blocking activity in a quasi-geostrophic model. *Tellus* **47A**, 941–954.

Lorenz E. N. 1963. Deterministic nonperiodic flow. *J. Atmos. Sci.* **20**, 130–141.

Malguzzi, P. 1993. An analytical study on the feedback between large- and small-scale eddies. *J. Atmos. Sci.* **50**, 1429–1436.

Marshall, J. and Molteni, F. 1993. Toward a dynamical understanding of planetary-scale flow regimes. *J. Atmos. Sci.* **50**, 1792–1818.

Michelangeli, P.-A., Vautard, R. and Legras, B. 1995. Weather regimes: recurrence and quasi-stationarity. *J. Atmos. Sci.* **52**, 1237–1256.

Mo, K.-C. and Ghil, M. 1988. Cluster analysis of multiple planetary flow regimes. *J. Geophys. Res.* **93**, 10927–10952.

Molteni, F., Sutera, A. and Tronci, N. 1988. EOFs of the geopotential eddies at 500 mb in winter and their probability density distributions. *J. Atmos. Sci.* **45**, 3063–3080.

Molteni, F., Tibaldi, S. and Palmer, T. N. 1990. Regimes in the winter-time circulation over northern extratropics. I: Observational evidence. *Q. J. R. Meteorol. Soc.* **116**, 31–67.

Namias, J. 1950. The index cycle and its role in the general circulation. *J. Meteor.* **7**, 130–139.

Palmer, T. N. 1999. A nonlinear dynamical perspective on climate prediction. *J. of Clim.* **12**, 575–591.

Pierrehumbert, R. T. and Malguzzi, P. 1984. Forced coherent structures and local multiple equilibria in a barotropic atmosphere. *J. Atmos. Sci.* **41**, 246–257.

Reinhold, B. and Pierrehumbert, R. T. 1982. Dynamics of weather regimes: quasi-stationary waves and blocking. *Mon. Weather Rev.* **110**, 1105–1145.

Renwick J. A. and Wallace J. M. 1996. Relationships between North Pacific Wintertime Blocking, El Niño, and the PNA pattern. *Mon. Weather Rev.* **124**, 2071–2075.

Rex, D. F. 1950a. Blocking action in the middle troposphere and its effect on regional climate. (I) An aerological study of blocking action. *Tellus* **2**, 196–211.

Rex, D. F. 1950b. Blocking action in the middle troposphere and its effect on regional climate. (II) The climatology of blocking action. *Tellus* **2**, 275–301.

Rossby, C.-G. et al. 1939. Relation between variations in the intensity of the zonal circulation in the atmosphere and the displacement of the semi-permanent centers of action. *J. Mar. Res.* **2**, 38–55.

Shutts, G. J. 1983. The propagation of eddies in diffluent jetstreams: eddy forcing of blocking flow fields. *Q. J. R. Meteorol. Soc.* **109**, 737–761.

Silverman, B. W. 1986. *Density estimation for statistics and data analysis.* Chapman and Hall, 175 pp.

Sutera, A. 1986. Probability density distribution of large scale atmospheric flow. *Adv. Geophys.* **29**, 319–338.

Tibaldi S. and Molteni, F. 1990. On the operational predictability of blocking. *Tellus* **42A**, 343–365.

Toth, Z. 1992. Quasi-stationary and transient periods in the Northern Hemisphere winter. *Mon. Weather Rev.* **119**, 1602–1611.

Tung, K. K. and Lindzen, R. S. 1979. A theory of stationary long waves. Part I: A simple theory of blocking. *Mon. Weather Rev.* **107**, 714–734.

Vautard, R. 1990. Multiple weather regimes over the North Atlantic. Analysis of precursor and successors. *Mon. Weather Rev.* **118**, 2056–2081.

Vautard, R. and Legras, B. 1988. On the source of low-frequency variability. Part II: Nonlinear equilibration of weather regimes. *J. Atmos. Sci.* **45**, 2845–2867.

Wallace, J. M. 1996. Observed climatic variability: Spatial structure. In: *Decadal climate variability — dynamics and predictability* (eds. D. L. T. Anderson and J. Willebrand). NATO ASI series, Vol. 44. Springer, 31–82.

Wallace, J. M. and Gutzler, D. S. 1981. Teleconnections in the geopotential height field during the northern hemisphere winter. *Mon. Weather Rev.* **109**, 784–81.

Wallace, J. M., Zhang Y. And Bajuk L. 1995. Interpretation of interdecadal trends in Northern Hemisphere surface air temperature. *J. of Clim.* **9**, 249–259.

Wiin-Nielsen, A. 1979. Steady states and stability proprieties of a low-order barotropic system with forcing and dissipation. *Tellus* **31**, 375–386.

Yang, S. and Reinhold, B. 1991. How does low-frequency variance vary? *Mon. Weather Rev.* **119**, 119–127.

Zorita, E. and Frankignoul, C. 1997. Modes of North Atlantic decadal variability in the ECHAM1/LSG coupled ocean–atmosphere general circulation model. *J. of Clim.* **10**, 183–200.